

Effective Photothermal Killing of Pathogenic Bacteria by Using Spatially Tunable Colloidal Gels with Nano-Localized Heating Sources

Chun-Wen Hsiao, Hsin-Lung Chen, Zi-Xian Liao, Radhakrishnan Sureshbabu, Hsu-Chan Hsiao, Shu-Jyuan Lin, Yen Chang,* and Hsing-Wen Sung*

Alternative approaches to treating subcutaneous abscesses—especially those associated with antibiotic-resistant pathogenic bacterial strains—that eliminate the need for antibiotics are urgently needed. This work describes a chitosan (CS) derivative with self-doped polyaniline (PANI) side chains that can self-assemble into micelles in an aqueous environment and be transformed into colloidal gels in a process that is driven by a local increase in pH. These self-doped PANI micelles can be utilized as nano-localized heat sources, remotely controllable using near-infrared (NIR) light. To test the *in vivo* efficacy of the CS derivative as a photothermal agent, an aqueous solution thereof is directly injected at the site of infected abscesses in a mouse model. The injected polymer solution eventually becomes distributed over the acidic abscesses, forming colloidal gels when it meets the boundaries of healthy tissues. After treatment with an 808 nm laser, the colloidal gels convert NIR light into heat, causing the thermal lysis of bacteria and repairing the infected wound without leaving residual implanted materials. This approach has marked potential because it can provide colloidal gels with tunable spatial stability, limiting localized heating to the infected sites, and reducing thermal damage to the surrounding healthy tissues.

1. Introduction

Subcutaneous abscesses are localized skin infections, which are typically caused by pathogenic bacteria native to the infected area of skin. Recently, methicillin-resistant *Staphylococcus aureus* (MRSA) has become a more common cause, presenting as more complex forms of subcutaneous infections.^[1] Clinically, the primary therapy for abscess management is incision and drainage, followed by systemic treatment with antibiotics. However, a patient on whom such a method is used suffers

from the pain that is associated with the surgical operation and, more importantly, the evolving bacterial resistance to antibiotics.^[2,3] Therefore, an urgent need exists to develop novel approaches that can eliminate both the incision/drainage procedure and the necessity to use antibiotics in treating subcutaneous abscesses.

The use of silver nanoparticles, which exhibit antimicrobial activities, has been proposed in the fight against various pathogenic organisms.^[4] However, the use of these silver nanoparticles as a bactericidal agent is considerably limited by their nonspecific biological toxicity.^[5] Another strategy involves using photothermal heat energy that is generated by gold, carbon, or graphene nanomaterials when exposed to near-infrared (NIR) light to activate the lysis of bacteria.^[6,7] The challenge in this method is the need of a suitable carrier to ensure the spatial stabilization of these nanomaterials to restrict the generated heat to the site of

abscesses. Nonlocalized heating commonly damages the surrounding healthy tissues.^[8]

This work reports an injectable polymer solution of a chitosan (CS) derivative containing self-doped polyaniline (PANI) side chains that can self-assemble to form nanoscale micelles in an aqueous environment and be transformed into colloidal gels *in situ* when the local pH changes. Notably, this pH-triggered colloidal-gel system undergoes a nanostructural transformation within a narrow pH range and can be spread over the acidic area of an abscess (pH 6.0–6.6)^[9] without overflowing onto the healthy tissues (pH 7.0–7.4).^[10] The self-doped PANI micelles within colloidal gels can then convert NIR light energy

Dr. C.-W. Hsiao, Prof. H.-L. Chen, Dr. R. Sureshbabu, S.-J. Lin,
Prof. H.-W. Sung
Department of Chemical Engineering
National Tsing Hua University
Hsinchu 30013, Taiwan (ROC)
E-mail: hwsung@mx.nthu.edu.tw
Prof. Z.-X. Liao
Institute of Medical Science and Technology
National Sun Yat-sen University
Kaohsiung, Taiwan (ROC)

DOI: 10.1002/adfm.201403478

H.-C. Hsiao, Prof. H.-W. Sung
Institute of Biomedical Engineering
National Tsing Hua University
Hsinchu 30013, Taiwan (ROC)
Dr. Y. Chang
Division of Cardiovascular Surgery
Veterans General Hospital–Taichung, College of Medicine
National Yang-Ming University
Taipei, Taiwan (ROC)
E-mail: ychang@vghtc.gov.tw



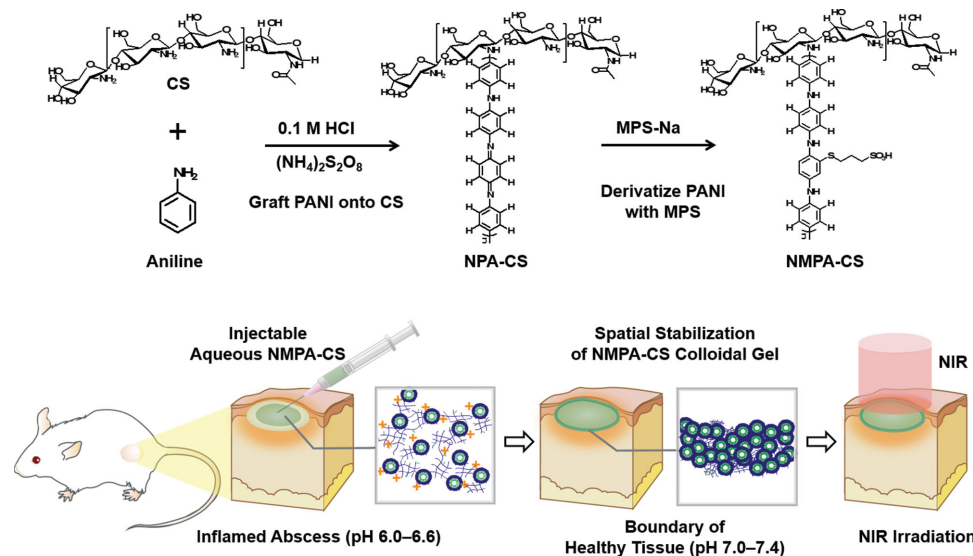


Figure 1. Developed procedure for synthesizing in situ-forming colloidal gel (NMPA-CS) and mechanism by which it treats subcutaneous abscess.

into heat, causing the thermal lysis of pathogenic bacteria. This approach has great potential because it can provide the tunable spatial stabilization of colloidal gels that are formed in situ, which limit localized heating to only the infected sites, reducing thermal damage to the surrounding healthy tissues (**Figure 1**).

CS is a biodegradable and tissue-compatible material.^[11] Since the pK_a of CS is 6.0–6.5, a pH-responsive hydrogelation may occur when it enters into a physiological environment (pH 7.0–7.4).^[12,13] PANI is one of the best characterized conducting polymers.^[14] Regarded as a non-cytotoxic material with high environmental stability, PANI has many biomedical applications.^[15] After doping by protons (i.e., protonation of the imine nitrogen atoms of PANI), PANI can absorb NIR light energy and generate a substantial amount of heat that can be utilized for cancer-cell ablation.^[16,17] Nevertheless, PANI loses its NIR photothermal activity over time in physiological pH environments owing to deprotonation or neutralization of these adsorbed protons, drastically limiting the range of clinical applications of PANI.^[16,18] To overcome this shortcoming, a self-doped PANI polymer is prepared and used herein.

The synthesized NPA-CS and NMPA-CS were characterized by Fourier transform infrared (FT-IR) and ^1H NMR spectroscopy. The FT-IR spectrum of NPA-CS exhibited two characteristic peaks at 1503 cm^{-1} and 1595 cm^{-1} , associated with the stretching vibrations of benzenoid and quinoid rings, respectively (**Figure 2a**). NMPA-CS had a strong absorption band at 1036 cm^{-1} , corresponding to the S=O stretching of the $-\text{SO}_3$ group that was present on the MPS substituent. In the ^1H NMR spectra (**Figure 2b**), a triplet was observed at 7.07 ppm ($J = 51.3$ Hz, characteristic of the coupling between ^1H and ^{14}N atoms) from the sample of NPA-CS and at 7.08 ppm ($J = 51.0$ Hz) from NMPA-CS, revealing the presence of protonated N-H groups ($-\text{N}^+\text{H}-$) on PANI.^[18] The above results verify that PANI was successfully grafted onto the free amine groups of CS (1, 2, 3, 4, 5, 6), but the degree of substitution

2. Results and Discussion

2.1. Characteristics of CS Derivative

The CS derivative was synthesized via a two-step reaction. Firstly, the graft of PANI onto CS (N-PANI-grafted CS; NPA-CS) was prepared by the in situ oxidative polymerization of aniline hydrochloride in the presence of $(\text{NH}_4)_2\text{S}_2\text{O}_8$ and CS (**Figure 1**). Then, a concurrent reduction and substitution (CRS) method was applied to derivatize the PANI backbone with mercaptopropylsulfonic acid (MPS), yielding the self-doped N-(MPS-substituted PANI)-CS (NMPA-CS).

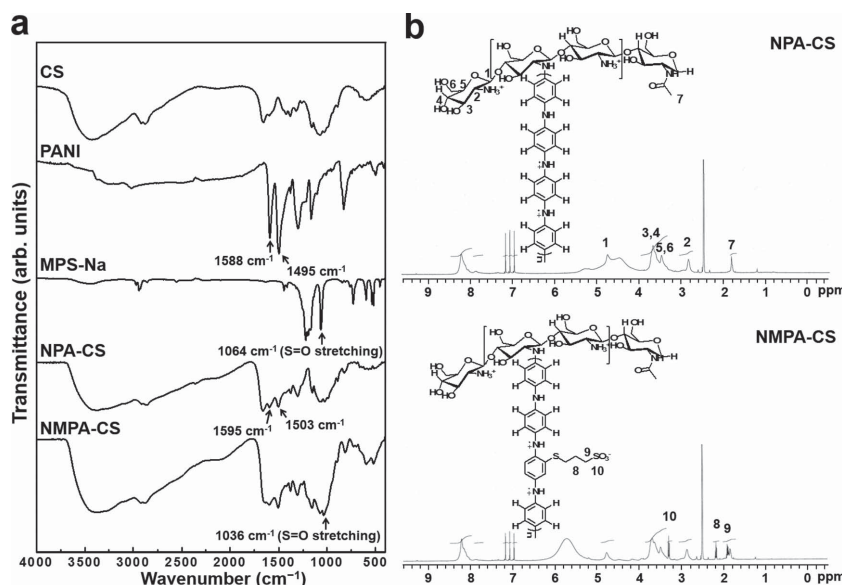


Figure 2. Results of analyses of synthesized copolymers: a) FT-IR spectra of CS, PANI, MPS-Na, NPA-CS, and NMPA-CS; b) ^1H NMR spectra of NPA-CS and NMPA-CS.

could not be calculated from the integral of the signal that was associated with the protonated amine groups of PANI (the triplet at ~ 7 ppm) because the ratio of their ionized groups is not known.^[19] Additionally, the appearance of alkyl protons in the spectrum of NMPA-CS suggests that the MPS group (8, 9, 10) was successfully conjugated to PANI.

2.2. Optical Property and Photostability of CS Copolymers

Owing to its low absorbance by tissue chromophores, NIR light can penetrate the skin to a depth of up to 10 mm without causing significant damage to blood or healthy tissues.^[20] Therefore, NIR light has been considered as one of the best ranges of wavelength of light for photothermal therapy that is focused on a targeted area of a subcutaneous tissue.^[21] The optical-absorbance peak of PANI is red-shifted toward the NIR region upon doping by protons, generating new energy levels between the valence and conduction bands, ultimately reducing the excitation-energy level and causing changes in color.^[22] As presented in Figure 3a, NPA-CS (the copolymer whose PANI side chains are not conjugated with MPS) was green (doped form) in a strongly acidic environment, but blue (undoped form) when its environmental pH approached the physiologic pH as a result of the deprotonation of PANI. Conversely, the self-doped copolymer (NMPA-CS) remained green throughout the pH range of interest, suggesting the stability of its optical properties. Additionally, at the physiological pH of 7.0, NMPA-CS absorbed much more strongly in the NIR biological window (750 to 1000 nm)^[23] than did NPA-CS (Figure 3b), making it useful for clinical applications. Therefore, NMPA-CS was selected for the following studies.

Owing to their “melting effect”, the NIR absorbance peak of gold nanorods, a widely known photothermal agent, is weakened by irradiating them with a laser for a certain period.^[24]

To test the photostability of NMPA-CS, an aqueous solution thereof at pH 7.0 was illuminated using a high-power NIR laser (808 nm, 4.0 W cm^{-2}) for particular periods. According to Figure 3c, no significant absorption changes were observed during a long period of exposure to the laser, suggesting the excellent photostability of NMPA-CS.

2.3. Supramolecular Structures of Aqueous NMPA-CS

The charged state of CS, as a polyelectrolyte, is governed by the pH of its environment.^[25] Grafting MPS-PANI onto the CS backbone (NMPA-CS) yields an amphiphilic copolymer, especially at low pH; the CS backbone is hydrophilic and its MPS-PANI side chains are hydrophobic. Notably, aqueous NMPA-CS thickened as its concentration was increased, forming a viscous solution. The effect of environmental pH on the supramolecular structures of NMPA-CS in an aqueous medium was examined by small-angle X-ray scattering (SAXS). Figures 4a,b present the relevant results, which are schematically presented in Figure 4c.

In Figure 4a, the two peaks in the blue curve, which was obtained by subtracting the SAXS profile of neat CS (the red curve) from that of NMPA-CS (the green curve), corresponded to the form factor maxima of micelles. In an aqueous medium, NMPA-CS with a high degree of substitution of MPS-PANI self-assembled to form supramolecular aggregates (such as micelles), in a process that was driven by the hydrophobic interaction of the substituted side chains. As shown by the black solid curve that is superposed on the experimental data, the subtracted profile was fitted closely by the form factor model of a core-shell sphere^[26] with a core diameter of around 65 nm and a shell thickness of approximately 0.6 nm. This experimental result was further verified by transmission electron microscopy (TEM; Figure 4d). A close examination

of the SAXS profiles in the high- q region ($q > 0.6 \text{ nm}^{-1}$) also revealed free CS chains with a low degree of grafting of MPS-PANI (Figure 4c).

Under acidic conditions, the micelles of NMPA-CS were uniformly distributed in the aqueous medium and loosely connected to each other via the free CS chains; the drastic increase in scattering intensity with the increase in the environmental pH to 7.0 is attributable to the aggregation of free CS chains and their associated micelles, owing to the deprotonation of the CS backbone, which was responsible for the hydrophobic character of the shells of the micelles (Figure 4b). Therefore, the gelation behavior of NMPA-CS can be attributed to an immediate change in the spatial distribution of the micelles from a state of more uniform dispersion to one of high aggregation, which constrains their mobility; this process is driven by the local increase in pH (Figure 4c). These results demonstrate that aqueous NMPA-CS can behave as an

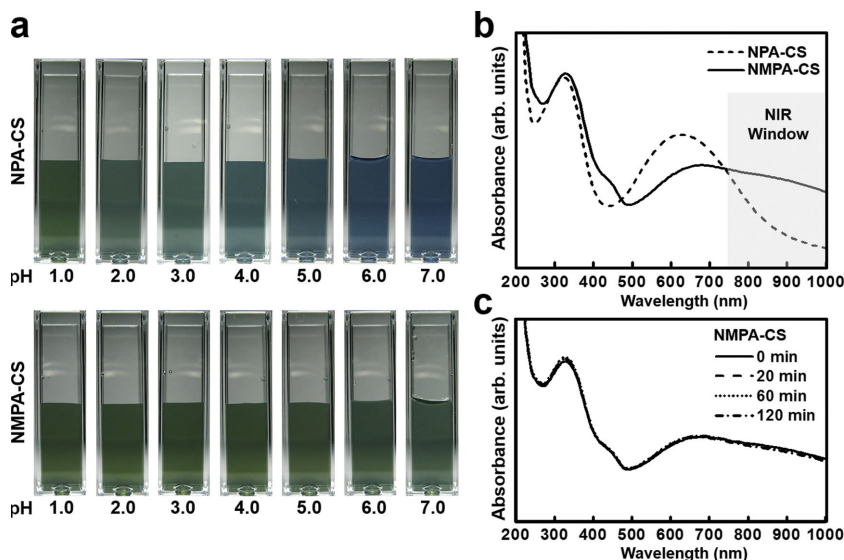


Figure 3. a) Photographs of aqueous NPA-CS and NMPA-CS solutions in environments with various pH values; b) UV-vis absorbance spectra of aqueous NPA-CS and NMPA-CS solutions at pH 7.0; c) changes in UV-vis absorbance spectra of aqueous NMPA-CS upon irradiation by NIR laser (4.0 W cm^{-2}) over time.

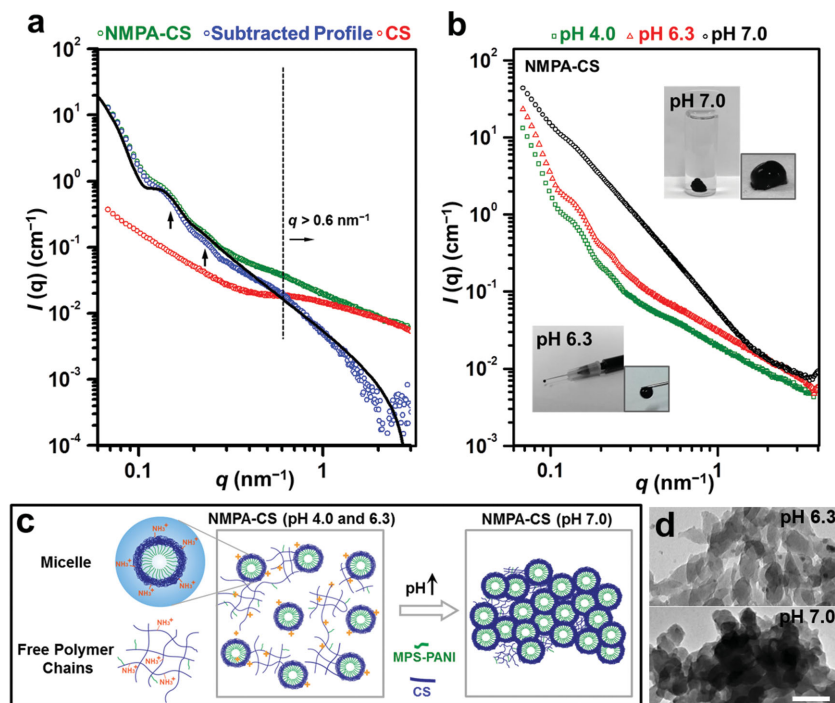


Figure 4. a) SAXS profiles of aqueous NMPA-CS (green curve) and neat CS (red curve) obtained at pH 4.0, and profile obtained from subtracting one from the other (blue curve) together with its fitted results (black solid curve); b) SAXS profiles and c) schematic supramolecular structures of aqueous NMPA-CS in environments with various pH values; d) TEM images of aqueous NMPA-CS at pH 6.3 and 7.0 (scale bar = 100 nm).

injectable and viscous fluid at low pH, and it undergoes hydrogelation immediately when the environmental pH is increased to 7.0 (see insets in Figure 4b).

The photothermal activity of NMPA-CS involves the side chains of the copolymer, MPS-substituted PANI, which form the core of the NMPA-CS micelles. Consequently, the micelles that are formed in the NMPA-CS colloidal gel can be used as nanoscale heat sources, which can be controlled remotely using NIR light. The transfer of heat from these micelles in the NMPA-CS colloidal gel heats the surrounding medium.

2.4. In Vitro Antibacterial Activity of NMPA-CS Micelles Mediated by NIR Light Irradiation

The antibacterial activity of NMPA-CS micelles, as a photothermal agent, against MRSA was characterized by performing a zone of inhibition (ZOI) test and a LIVE/DEAD bacterial viability assay. In the ZOI study, various concentrations of aqueous NMPA-CS were mixed with Mueller-Hinton agar and allowed to complete gelation. Each as-prepared agar-gel was then exposed to an 808 nm NIR laser (2.0 W cm^{-2}); temperature profiles and heat maps of the gels

were obtained using an infrared (IR) thermal camera. Following exposure to NIR light, the temperature of each studied agar-gel that contained NMPA-CS micelles was increased rapidly (Figure 5a). The increase in temperature depended strongly on the concentration of NMPA-CS that was mixed in the agar-gels, suggesting that NMPA-CS micelles may act as an efficient photothermal agent.

Following laser treatment, the heat map of the agar-gel with $200 \mu\text{g mL}^{-1}$ NMPA-CS showed a core central region with a maximum temperature of approximately 55°C , surrounded by zones with a large temperature gradient (Figure 5b), which favors localized heat treatment.^[2] Above 50°C , the enzymes in bacteria become denatured and their proteins and lipids on the cell membranes are damaged, eventually causing bacterial death.^[7] The ZOI test was conducted involved lawn cultures of MRSA at a concentration of 10^8 colony forming units (CFU) mL^{-1} , grown on the agar-gel with $200 \mu\text{g mL}^{-1}$ NMPA-CS. The agar that contained no NMPA-CS served as a control. The tested agar-gels were separately irradiated by the aforementioned NIR laser beam for specified periods and then placed in an incubator. Subsequent to incubation for 24 h at 37°C , the test plates were photographed and then analyzed using an image software system to determine the ZOIs of bacteria or the zones of clearance.

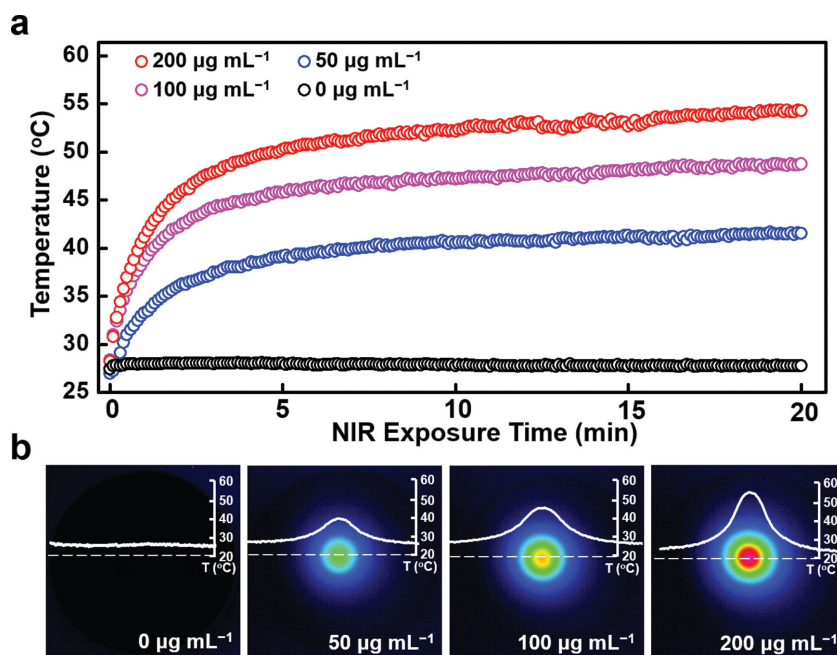


Figure 5. a) Temperature evolution curves of agar-gels that contained different concentrations of NMPA-CS (0, 50, 100, $200 \mu\text{g mL}^{-1}$) when exposed to NIR laser (2.0 W cm^{-2}) and b) their thermographic images at end of period of laser treatment.

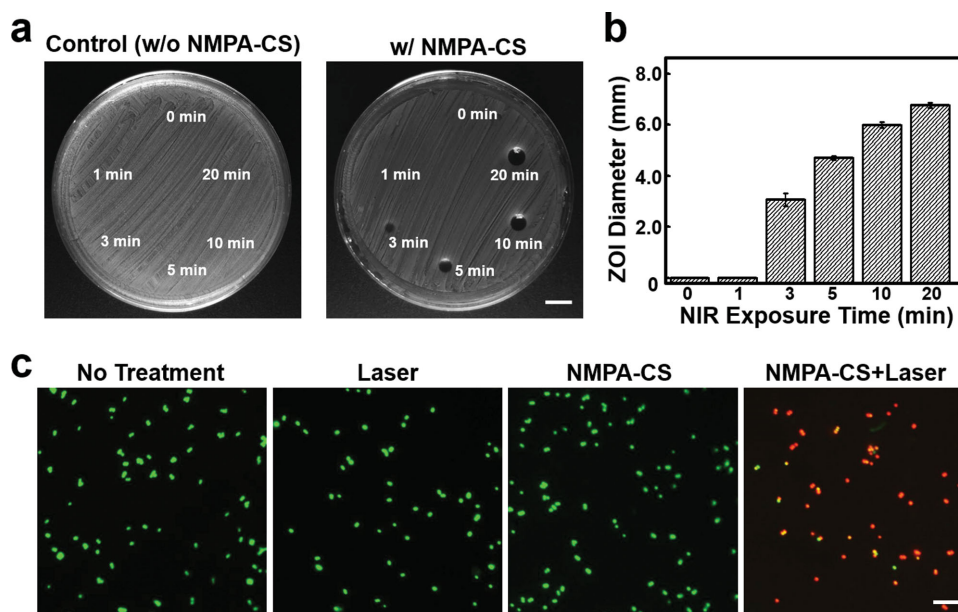


Figure 6. In vitro antibacterial activities of NMPA-CS micelles mediated by NIR light irradiation: a) photographs and b) diameters of ZOIs of test agar-gel (containing $200 \mu\text{g mL}^{-1}$ NMPA-CS; $n = 6$) that was exposed to NIR laser (2.0 W cm^{-2}) for particular periods. Agar without NMPA-CS was a control (scale bar = 10 mm); c) live (green fluorescence) and dead (red fluorescence) stained MRSA following various treatments (scale bar = 10 μm).

In **Figure 6a**, no zone of clearance was apparent in the control agar plate (left panel) following 20 min of exposure to the NIR laser, suggesting that the NIR light did not have any bactericidal effect. Conversely, in the agar plate that contained NMPA-CS (right panel), zones of clearance were clearly observed at locations that had been exposed to the laser light. The light from the NIR laser that was absorbed by NMPA-CS micelles was efficiently converted into localized heat, destroying the bacteria. The diameter of ZOIs increased along with exposure to NIR, reaching the width of the laser light (approximately 6.5 mm) after 20 min of exposure (**Figure 6b**), indicating the complete photothermal lysis of the bacteria.

To confirm further the effectiveness of NMPA-CS micelles as a photothermal agent, MRSA was suspended in an aqueous solution of NMPA-CS at a concentration of $200 \mu\text{g mL}^{-1}$ and then irradiated by the 808 nm NIR laser. The untreated MRSA and those exposed to the laser light alone or with treatment with NMPA-CS only were the controls. Twenty minutes after each treatment, test bacteria were collected via centrifugation, and their viability was evaluated using a LIVE/DEAD BacLight Bacterial Viability Kit. With this kit, live bacteria with intact cell membranes were stained fluorescent green while dead bacteria with damaged membranes were stained fluorescent red.^[27] These results were analyzed using imaging software and represented as percentage cell viability.^[5]

From **Figure 6c**, the test bacteria in the control groups mainly emitted green fluorescence (>96% live cells), suggesting that treatment with laser or NMPA-CS alone negligibly affected the viability of bacteria. However, the exposure of MRSA to NIR light in the presence of NMPA-CS micelles greatly increased the number of dead or compromised cells, as indicated by the prevalence of “red” dead cells (<6% live cells). These results revealed the feasibility of using NMPA-CS micelles as a photothermal agent to reduce the viability of bacteria following exposure to NIR.

2.5. Tunable Spatial Stabilization of NMPA-CS Colloidal Gel

One of the main challenges in thermal therapy is to local restriction of heating at the diseased sites without damaging the surrounding healthy tissue.^[28] Since subcutaneous abscesses have reduced pH,^[9] an agent that both is pH-responsive and has photothermal properties, such as the developed NMPA-CS colloidal gel, can be used to restrict heating to sites of infection. As demonstrated in vitro in **Figure 7**, a droplet of such a viscous NMPA-CS solution (30 mg mL^{-1}) in an environment of pH 6.3 could spread gradually over the local surface in a period of 1 h, but it retained its original shape in an environment with a pH of 7.0. Given this unique pH-responsive feature, aqueous NMPA-CS may behave as a viscous fluid and become distributed over acidic abscesses (pH 6.0–6.6) over time; when it encounters a boundary of a healthy tissue (pH 7.0–7.4), NMPA-CS

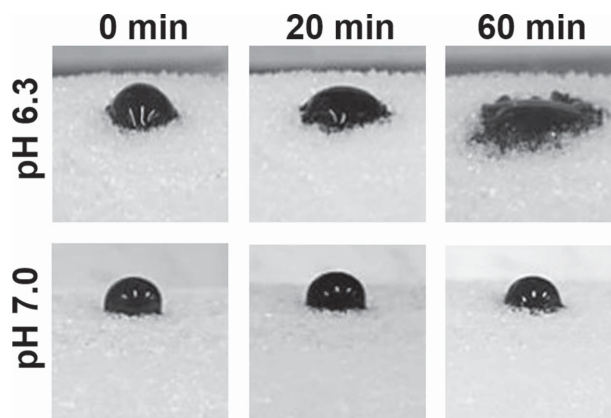


Figure 7. Changes in morphology of an aqueous NMPA-CS droplet on surface of sponge that had been presoaked in a buffer of pH 6.3 or 7.0.

may respond to the locally increased pH by changing its physical shape and by rapidly forming colloidal gels without flowing over the neighboring healthy tissues.

2.6. In Vivo Antibacterial Activity of NMPA-CS Colloidal Gel Mediated by NIR Light Irradiation

To test the efficacy of NMPA-CS as a photothermal agent in vivo, a subcutaneous abscess was experimentally created in a mouse model via the local injection of MRSA (10^7 CFU mL⁻¹, 100 μ L). Twenty-four hours later, an infected wound formed subcutaneously (as indicated by the black arrow in the left panel in Figure 8a); an aqueous NMPA-CS solution (30 mg mL⁻¹, 100 μ L; pH 6.3) was then injected at the site of infection through a 25G needle.

One hour following injection with NMPA-CS, the heating effect of the colloidal gels that were formed in situ was examined using an IR thermal camera. During NIR irradiation (0.5 W cm^{-2} for 20 min), the lenses of the laser were dynamically adjusted to vary the size of the laser spot such that it covered the entire abscess. According to the obtained thermographic images (the middle panel in Figure 8a), only the region in which NMPA-CS and NIR light were both present exhibited a sharp rise in temperature to approximately 55 °C in just 5 min; this temperature was sufficiently high to kill bacteria,

as demonstrated in the in vitro study (Figure 6a). Whereas the tissue that surrounded NMPA-CS exhibited a mild temperature increase to about 40 °C, no significant temperature change was observed on other parts of the mouse. Subsequent to the thermal analysis, the mice were sacrificed and their skins were exposed. Most of the NMPA-CS colloidal gel that formed in situ was at the site of the abscess (with a coverage ratio of around 90%; as denoted by the white arrow in the right panel in Figure 8a), which was the region where a significant increase in temperature had been observed in the thermographic images.

The bactericidal effect of the NMPA-CS colloidal gels that formed in mice ($n = 6$) with subcutaneous abscesses upon exposure to an 808 nm laser was investigated. Each mouse received four bacterial injections, which developed into four infected wounds within 24 h and these were treated under one of four experimental conditions – untreated control, exposed to laser alone, injected with NMPA-CS only, and treated with NMPA-CS and exposed to a laser. On day one after treatment, abscess tissues were excised and homogenized. The bactericidal effect in each test group of mice was then examined by determining the number of CFUs in the homogenate using standard plate counting methods (Figure 8b).^[29] The CFU count for each treatment modality was normalized by dividing by the CFU count for the untreated wound (Figure 8c). The CFU counts in Figures 8b and 8c revealed a strong antibacterial effect on the

infected wound associated with the subcutaneous abscess that received NMPA-CS and was exposed to the NIR laser, reducing the CFU count to approximately 18% of those of the wounds that had been treated with the laser or NMPA-CS alone ($P < 0.05$). On day seven after treatment, the skin of the mice that had been treated with both NMPA-CS and the laser was healed and had formed a scab, resulting from the biological process of wound repair; the scab and the implanted NMPA-CS colloidal gel flaked off within ten days (Figure 8d). In the mice that had undergone no treatment, inflamed tissues were still observed subcutaneously.

The healing of the infected wounds that had been photothermally treated with both NMPA-CS and the NIR laser was further verified by histological analyses of skin sections that were stained with hematoxylin–eosin (H&E). A comparison with the healthy control revealed signs of severe infection before treatment, while a markedly reduced infiltration of inflammatory cells was seen following the photothermal treatment with NMPA-CS (Figure 8e), implying its strong bactericidal effect. The in vivo biocompatibility of NMPA-CS was also evaluated in the study using a mouse model. At four weeks post-implantation, only a mild foreign-body reaction (fibroblasts with intermingling inflammatory cells, indicated by the black arrow in Figure 8f) was observed in the peri-implant tissue.

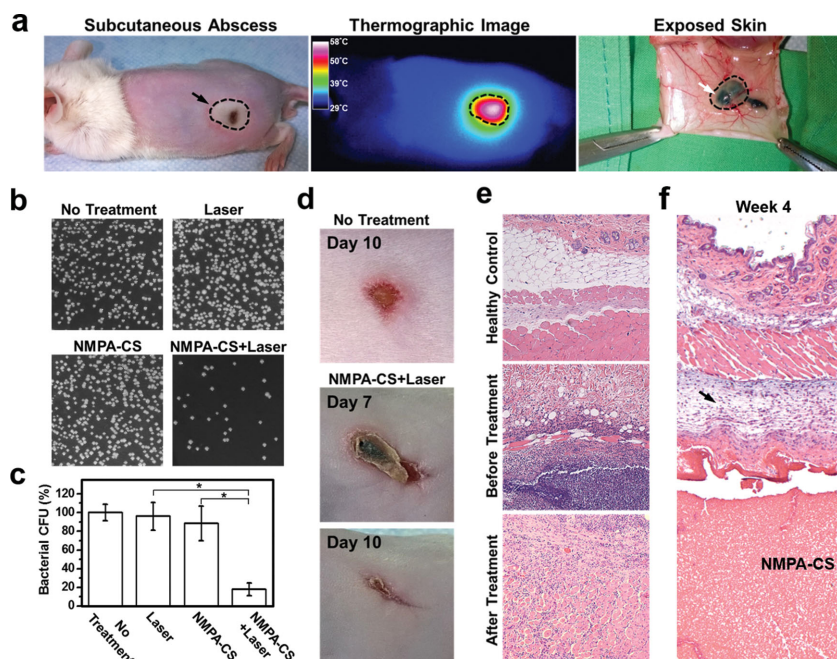


Figure 8. a) A mouse with a subcutaneous abscess before treatment, its thermographic image following treatment by NMPA-CS and exposure to laser light, and its exposed skin following treatment; b) photomicrographs of bacterial CFU, obtained from infected tissues of mice that had been treated under various experimental conditions and c) related quantitative results ($n = 6$); d) photographs of infected skin of untreated mice and mice following NMPA-CS + laser treatment; e) histological photomicrographs of skin tissue sections of infected mice before and after NMPA-CS + laser treatment (on day 10). Mice with healthy skin tissue served as a control; f) histological photomicrographs of NMPA-CS colloidal gel and its surrounding tissue that were retrieved at four weeks after implantation. All sections were stained with H&E. *Statistical significance at $P < 0.05$.

3. Conclusion

In summary, an in situ-forming colloidal gel that can provide tunable spatial stabilization over the acidic area of subcutaneous abscesses without overflowing onto the healthy tissue was successfully prepared. The formed colloidal gel effectively converted NIR light energy into localized heat, causing the thermal lysis of bacteria and repairing the infected wound without leaving residual implanted materials. The minimally invasive method described here, which does not involve conventional antibiotics, has great potential in the treatment of subcutaneous infections against pathogenic bacteria, including antibiotic-resistant strains. This treatment platform may be extended to other clinical needs, and especially localized hyperthermia-based cancer therapy.

4. Experimental Section

Materials: CS (viscosity 36 mPa s, 0.5% in 0.5% acetic acid at 20 °C) with approximately 85% deacetylation was purchased from Koyo Chemical Co. Ltd. (Tokyo, Japan). Aniline, ammonium persulfate (APS), hydrochloric acid (HCl), sodium hydroxide (NaOH), 1-methyl-2-pyrrolidinone (NMP), and 3-mercapto-1-propanesulfonic acid sodium salt (MPS-Na) were obtained from Sigma-Aldrich (St Louis, MO, USA). All other chemicals and reagents were analytical grade. The MRSA strain used in the study was provided by the Clinical Microbiology Laboratory, National Taiwan University Hospital, Hsinchu Branch (Taiwan).

Synthesis of NPA-CS and NMPA-CS Copolymers: An aqueous mixture of CS (2 g) and HCl (0.1 M, 900 mL) was prepared and stirred overnight to ensure complete dissolution. Aniline (14.5 mM) was subsequently added to the CS solution; following solubilization, equimolar of APS was introduced into the mixed solution. The polymerization of PANI on CS (NPA-CS copolymer) was carried out for 3 h in an ice bath. The as-prepared NPA-CS copolymer was then neutralized and precipitated by adjusting its pH value to 8.0 using NaOH; free PANI was removed with NMP. NMPA-CS (the copolymer with MPS conjugated on its PANI side chains) was prepared by reacting NPA-CS (1 g) with 0.1 M MPS-Na in deionized (DI) water (150 mL) in an atmosphere of N₂ for 14 h to allow for the completion of the CRS reaction.^[30] A catalytic amount of acetic acid (0.01 M) was added to accelerate the reaction. The resultant copolymer (NMPA-CS) was precipitated by NaOH, washed with an excess of DI water, and then air-dried.

Analyses of Synthesized Copolymers: The chemical structures of the synthesized copolymers were analyzed by FT-IR (Perkin-Elmer, Buckinghamshire, UK) and ¹H NMR (Varian Unity Inova 500, Missouri, USA) spectroscopy. The ¹H NMR spectra of test samples were recorded at 25 °C in DMSO-d₆ to which a few drops of acid had been added.^[19] The UV-vis optical properties of the copolymers in phosphate-buffered saline were studied using a SpectraMax M5 Microplate Reader (Molecular Devices, Sunnyvale, CA, USA).

Supramolecular Structures of Aqueous NMPA-CS: SAXS was utilized to probe the transformation of the supramolecular structures that were associated with the hydrogelation of aqueous NMPA-CS (30 mg mL⁻¹) in environments with various pH values. The experiments were performed using the BL23A1 beamline at the National Synchrotron Radiation Research Center (NSRRC), Hsinchu, Taiwan. The energy of the beam source was 15 keV, and the sample-to-detector distance was 3060.3 mm. The scattering signals were collected by a MarCCD detector with a pixel resolution of 512 × 512. The scattering intensity profile was obtained as a plot of scattering intensity *I*(*q*) as a function of scattering vector, *q* = (4π/λ)sin(θ/2) (θ = scattering angle), after corrections for sample transmission, empty cell transmission, empty cell scattering, and the sensitivity of the detector.^[12] The SAXS profile determined by the form factor of the micelles that were assembled by NMPA-CS was

fitted by the core-shell sphere model,^[26] using the program that was provided by the Center for Neutron Research at the National Institute of Standards and Technology, Gaithersburg, Maryland. The model considers the polydispersity of the core radius, given a size distribution that is described by the Schultz distribution function. Owing to the presence of residual free CS, both NMPA-CS micelles and free CS chains contributed to the SAXS profile of the experimentally obtained solution. The scattering contributed by the micelles was obtained by subtracting the SAXS profile of neat CS from that of NMPA-CS with the application of an appropriate weighting factor. For TEM observation, NMPA-CS micelles were stained using OsO₄ to give the dark contrast of PANI and CS.^[12,31] TEM images were then obtained under a JEOL-1010 microscope (Akishima, Tokyo, Japan) with an accelerating voltage of 100 kV.

Antibacterial Activity of NMPA-CS: The in vitro antibacterial activity of NMPA-CS was evaluated based on the principle of the Kirby-Bauer assay.^[2] MRSA suspensions (10⁸ CFU mL⁻¹) were swabbed onto the agar-gel (NMPA-CS) plates and then exposed to NIR laser light (808 nm, Tanyu Tech., Taiwan) for varying periods, before being incubated for 24 h at 37 °C to allow lawn growth. Immediately following incubation, the diameters of the ZOI were determined in mm using Image-Pro Plus software (Version 4.5, Media Cybernetics, Bethesda, MD, USA). In the LIVE/DEAD bacterial viability assay, test samples were stained with a 0.85% NaCl solution that contained 5 μM of green-fluorescing SYTO 9 and 30 μM of red-fluorescing propidium iodide (Invitrogen, Carlsbad, CA, USA) for 20 min at room temperature. Samples were visualized under a fluorescence microscope (Axio Observer Z1, Zeiss, Göttingen, Germany).

Animal Studies: ICR mice (eight weeks old) were used in the animal study. Animal care and use complied with the "Guide for the Care and Use of Laboratory Animals", prepared by the Institute of Laboratory Animal Resources, National Research Council, and published by the National Academy Press (1996). The Institutional Animal Care and Use Committee of National Tsing Hua University (Hsinchu, Taiwan) approved the study protocol (#10258). To evaluate the efficacy of the NMPA-CS colloidal gel as a photothermal agent, a subcutaneous abscess was experimentally created in each test mouse. Briefly, the mice were firstly anesthetized using 2% isoflurane with oxygen. After shaving and disinfection, a subcutaneous injection of MRSA (10⁷ CFU mL⁻¹, 100 μL) was given on the shaved back of the test animals. Six mice were used in this study. At 24 h following the injection of bacteria, an infected abscess had formed subcutaneously in each test mouse; a polymer solution of NMPA-CS (30 mg mL⁻¹, pH 6.3) was then directly injected into the infected wound. An 808 nm laser (0.5 W cm⁻²) was used to illuminate the NMPA-CS colloidal gel that was formed in situ. During the 20 min of laser irradiation, the animals were under anesthesia. The thermographic images of each test animal were then recorded by an IR thermal camera (ICI7320, Infrared Camera, Beaumont, TX, USA). Following the thermographic analysis, the mice were euthanized by CO₂ inhalation, and their skins were exposed and photographed. To investigate their bactericidal effects, each test mouse received four MRSA infections, and these were then treated under one of the following four experimental conditions; no treatment; exposed to the laser alone; injected with only NMPA-CS; and treated with NMPA-CS and exposed to the laser (n = 6). Following treatments, the mice were sacrificed and the infected tissues were harvested and analyzed by histological and standard plate count methods.

Statistical Analysis: All results are presented as mean ± SD. The Student *t* test was performed to compare the means of pairs of groups. One-way ANOVA was followed by the Bonferroni *post hoc* test to compare three or more groups. Differences were regarded as statistically significant at *P* < 0.05.

Acknowledgements

The authors would like to thank the National Science Council of the Republic of China, Taiwan, for financially supporting this research

under Contract Nos. NSC 103–2221-E-007–022-MY3 and NSC 103–2120-M-007–009-CC1.

Received: October 5, 2014

Revised: October 31, 2014

Published online: December 8, 2014

- [1] A. P. Ladd, M. S. Levy, J. Quilty, *J. Pediatr. Surg.* **2010**, *45*, 1562.
- [2] N. Kojic, E. M. Pritchard, H. Tao, M. A. Brenckle, J. P. Mondia, B. Panilaitis, F. Omenetto, D. L. Kaplan, *Adv. Funct. Mater.* **2012**, *22*, 3793.
- [3] a) S. Iyer, D. H. Jones, *J. Am. Acad. Dermatol.* **2004**, *50*, 854; b) S. B. Levy, B. Marshall, *Nat. Med.* **2004**, *10*, S122.
- [4] a) A. Agarwal, K. M. Guthrie, C. J. Czuprynski, M. J. Schurr, J. F. McNulty, C. J. Murphy, N. L. Abbott, *Adv. Funct. Mater.* **2011**, *21*, 1863; b) C. P. Chen, P. Gunawan, X. W. Lou, R. Xu, *Adv. Funct. Mater.* **2012**, *22*, 780; c) Z. J. Fan, B. Liu, J. Q. Wang, S. Y. Zhang, Q. Q. Lin, P. W. Gong, L. M. Ma, S. R. Yang, *Adv. Funct. Mater.* **2014**, *24*, 3933.
- [5] R. S. Norman, J. W. Stone, A. Gole, C. J. Murphy, T. L. Sabo-Attwood, *Nano Lett.* **2008**, *8*, 302.
- [6] a) W. C. Huang, P. J. Tsai, Y. C. Chen, *Small* **2009**, *5*, 51; b) X. Dong, Y. Tang, M. Wu, B. Vlahovic, L. Yang, *J. Biol. Eng.* **2013**, *7*, 19.
- [7] M. C. Wu, A. R. Deokar, J. H. Liao, P. Y. Shih, Y. C. Ling, *ACS Nano* **2013**, *7*, 1281.
- [8] T. S. Hauck, T. L. Jennings, T. Yatsenko, J. C. Kumaradas, W. C. W. Chan, *Adv. Mater.* **2008**, *20*, 3832.
- [9] a) A. Lardner, *J. Leukocyte Biol.* **2001**, *69*, 522. b) C. W. Ford, J. C. Hamel, D. Stapert, R. J. Yancey, *J. Med. Microbiol.* **1989**, *28*, 259.
- [10] J. Panyam, Y. Patil, *Preclinical Development Handbook: ADME and Biopharmaceutical Properties* (Eds: S. C. Gad), Wiley, Hoboken, NJ, USA **2008**, Ch. 10.
- [11] C. A. Custodio, V. E. Santo, M. B. Oliveira, M. E. Gomes, R. L. Reis, J. F. Mano, *Adv. Funct. Mater.* **2014**, *24*, 1391.
- [12] Y. L. Chiu, S. C. Chen, C. J. Su, C. W. Hsiao, Y. M. Chen, H. L. Chen, H. W. Sung, *Biomaterials* **2009**, *30*, 4877.
- [13] Y. L. Chiu, M. C. Chen, C. Y. Chen, P. W. Lee, F. L. Mi, U. S. Jeng, H. L. Chen, H. W. Sung, *Soft Matter* **2009**, *5*, 962.
- [14] S. Virji, R. B. Kaner, B. H. Weiller, *Chem. Mater.* **2005**, *17*, 1256.
- [15] a) T. G. Kim, H. Shin, D. W. Lim, *Adv. Funct. Mater.* **2012**, *22*, 2446; b) D. Y. Zhai, B. R. Liu, Y. Shi, L. J. Pan, Y. Q. Wang, W. B. Li, R. Zhang, G. H. Yu, *ACS Nano* **2013**, *7*, 3540; c) C. W. Hsiao, M. Y. Bai, Y. Chang, M. F. Chung, T. Y. Lee, C. T. Wu, B. Maiti, Z. X. Liao, R. K. Li, H. W. Sung, *Biomaterials* **2013**, *34*, 1063; d) G. Thiruvikraman, G. Madras, B. Basu, *Biomaterials* **2014**, *35*, 6219; e) L. Cheng, C. Wang, L. Feng, K. Yang, Z. Liu, *Chem. Rev.* DOI: 10.1021/cr400532z.
- [16] J. Yang, J. Choi, D. Bang, E. Kim, E. K. Lim, H. Park, J. S. Suh, K. Lee, K. H. Yoo, E. K. Kim, Y. M. Huh, S. Haam, *Angew. Chem. Int. Ed.* **2011**, *50*, 441.
- [17] J. Zhou, Z. G. Lu, X. J. Zhu, X. J. Wang, Y. Liao, Z. F. Ma, F. Y. Li, *Biomaterials* **2013**, *34*, 9584.
- [18] S. L. Mu, *Synth. Met.* **2010**, *160*, 1931.
- [19] P. Marcasuzaa, S. Reynaud, F. Ehrenfeld, A. Khoukh, J. Desbrieres, *Biomacromolecules* **2010**, *11*, 1684.
- [20] D. O. Lapotko, *Theranostics* **2013**, *3*, 138.
- [21] D. P. O'Neal, L. R. Hirsch, N. J. Halas, J. D. Payne, J. L. West, *Cancer Lett.* **2004**, *209*, 171.
- [22] J. Park, D. Bang, K. Jang, S. Haam, J. Yang, S. Na, *Nanotechnology* **2012**, *23*, 365705.
- [23] a) M. Nyk, R. Kumar, T. Y. Ohulchanskyy, E. J. Bergey, P. N. Prasad, *Nano Lett.* **2008**, *8*, 3834; b) J. Zhou, Y. Sun, X. X. Du, L. Q. Xiong, H. Hu, F. Y. Li, *Biomaterials* **2010**, *31*, 3287.
- [24] a) K. Yang, H. Xu, L. Cheng, C. Y. Sun, J. Wang, Z. Liu, *Adv. Mater.* **2013**, *25*, 945; b) Z. B. Zha, X. L. Yue, Q. S. Ren, Z. F. Dai, *Adv. Mater.* **2013**, *25*, 777.
- [25] N. Bhattarai, J. Gunn, M. Q. Zhang, *Adv. Drug Deliver. Rev.* **2010**, *62*, 83.
- [26] L. A. Feigin, D. I. Svergun, *Structure Analysis by Small-Angle X-Ray and Neutron Scattering* (Eds: G. W. Taylor), Plenum Press, New York **1987**.
- [27] S. M. Kang, N. S. Hwang, J. Yeom, S. Y. Park, P. B. Messersmith, I. S. Choi, R. Langer, D. G. Anderson, H. Lee, *Adv. Funct. Mater.* **2012**, *22*, 2949.
- [28] M. Babincova, D. Leszczynska, P. Sourivong, P. Cicmanec, P. Babinec, *J. Magn. Magn. Mater.* **2001**, *225*, 109.
- [29] D. G. Saymen, P. Nathan, I. A. Holder, E. Hill, B. G. Macmillan, *Appl. Microbiol.* **1972**, *23*, 509.
- [30] C. C. Han, C. H. Lu, S. P. Hong, K. F. Yang, *Macromolecules* **2003**, *36*, 7908.
- [31] B. Nandan, J. Y. Hsu, A. Chiba, H. L. Chen, C. S. Liao, S. A. Chen, H. Hasegawa, *Macromolecules* **2007**, *40*, 395.